



CGU HS Committee on River Ice Processes and the Environment
13th Workshop on the Hydraulics of Ice Covered Rivers
Hanover, NH, September 15-16, 2005

**Hydrodynamic Characteristics of Waves Released by
Ice Cover Consolidation and Effects on Ice Cover Stability
of Peace River below Dunvegan**

Spyros Beltaos

*National Water Research Institute, Environment Canada,
867 Lakeshore Road, Burlington, ON, L7R 4A6, Canada
spyros.beltaos@ec.gc.ca*

David D. Andres

*Northwest Hydraulic Consultants, 4823-99th Street,
Edmonton, AB, T6E 4Y1, Canada
dandres@nhc-edm.com*

Ice consolidations during freeze-up on the Peace River (Alberta) can produce local flooding due to either the attendant surge of ice and water or the resulting over-thickened ice accumulation. These consolidation events occur very quickly, they affect the ice cover over a relatively short domain of the river, but produce steep waves that are felt a long distance downstream. The available evidence suggests a link between certain types of consolidation with sharp temperature increases. Although the impacts of such events have been measured, there is limited knowledge of how they are initiated, and of the hydrodynamic characteristics and ice-breaking capacity of the resulting waves. The issue of climate change and variability underscores the need for improved understanding of consolidation-generated waves.

In 2000-01, a consolidation event was detected on the Peace River between Dunvegan and the Town of Peace River. The response of the Dunvegan gauge upstream of the consolidation provided an indication of the rate at which the ice cover collapsed, and three gauges downstream of the consolidation measured the resulting water wave. Using a recently-developed analytical method that is based on the one-dimensional equations of motion, flow velocity, discharge, and boundary shear stress were determined for the waveform. These values are in agreement with earlier estimates that were obtained via numerical modelling. Using the calculated shear stress values, the capacity of the wave to dislodge the solid-ice cover is examined within the context of the existing criteria of breakup initiation. The resulting inferences compare favourably to observations.

1. Introduction

The stability of an ice cover on regulated rivers in Canada is one of the major operational constraints to winter generation of hydroelectric power (Wigle et al., 1990). Hydropower production typically leads to an increase in discharge at freeze-up, often resulting in a more dynamic freeze-up than would occur naturally. In western Canada, this is an issue at least on the Bow, North Saskatchewan, Peace, and Nechako Rivers. Observations indicate that consolidation events, which comprise the collapse and thickening of a newly formed ice cover, cause some of the highest winter water levels. These consolidation processes are most evident on the Peace River, where regulation has had the most dramatic effect on winter flows – discharges at freeze-up have been increased by about 400%, relative to the pre-regulated condition.

Neill and Andres (1984) documented one significant consolidation event that occurred on the Peace River in 1981 when almost 100 km of newly-formed ice cover collapsed into about 40 km of rubble, raising water levels at the Town of Peace River (TPR) to near-record levels. Their analysis showed that the stage increase at the town was due to an increase in the thickness of the ice cover and to the effects of a water wave that was abruptly released from channel storage during the collapse. While the effects of the wave were short lived, the effects of the thicker ice cover persisted for the entire winter.

More recently, Andres et al. (2003) described a Peace-River collapse event that took place near Dunvegan on February 27, 2001, at ~ 1930 h. A rise in mean daily air temperature, from -23.6°C on February 25 to -3.0°C on February 27 preceded the collapse. About 27 km of ice cover was consolidated into some 13 km of rubble. After the collapse, the head of the ice cover was located at km 923, and the toe of the now thickened accumulation was located at km 910, or about 9 km upstream of the gauge at Elk Island (Fig.1).

Andres et al. (2003) pointed out that there is little quantitative information in the literature about this phenomenon. They suggested that to quantify the effects of a consolidation and to forecast the likelihood and the outcome of its occurrence requires a thorough understanding of: (a) triggering of the event; (b) release of water upon collapse of the ice cover; (c) hydrodynamic characteristics of the water wave as it advances ahead of the moving ice; (d) downstream translation and thickening of the ice cover; and (e) eventual arrest of the moving rubble against the solid ice cover downstream. One of the simpler of the above issues, the pattern of water release from storage was addressed by Andres et al. (2003) who inferred the outflow hydrograph that was generated by the consolidation event, based on measured water waves at three gauge sites downstream of the consolidation reach. The authors also noted that the original ice cover downstream of the re-formed accumulation remained largely intact (Fig. 1), despite being subjected to relatively large shear stresses and water-level increases of up to four times the thickness of the thermal (solid) ice in the accumulation.

Herein, a recently-developed analytical method is utilized to (a) deduce important hydraulic characteristics of the measured waveforms, such as peak discharge, flow velocity, and shear stress; (b) compare the results with corresponding values deduced by Andres et al. (2003) using numerical modelling; and (c) use these findings to examine the capacity of the water wave to dislodge the solid-ice cover, within the context of physically-based criteria of breakup initiation.

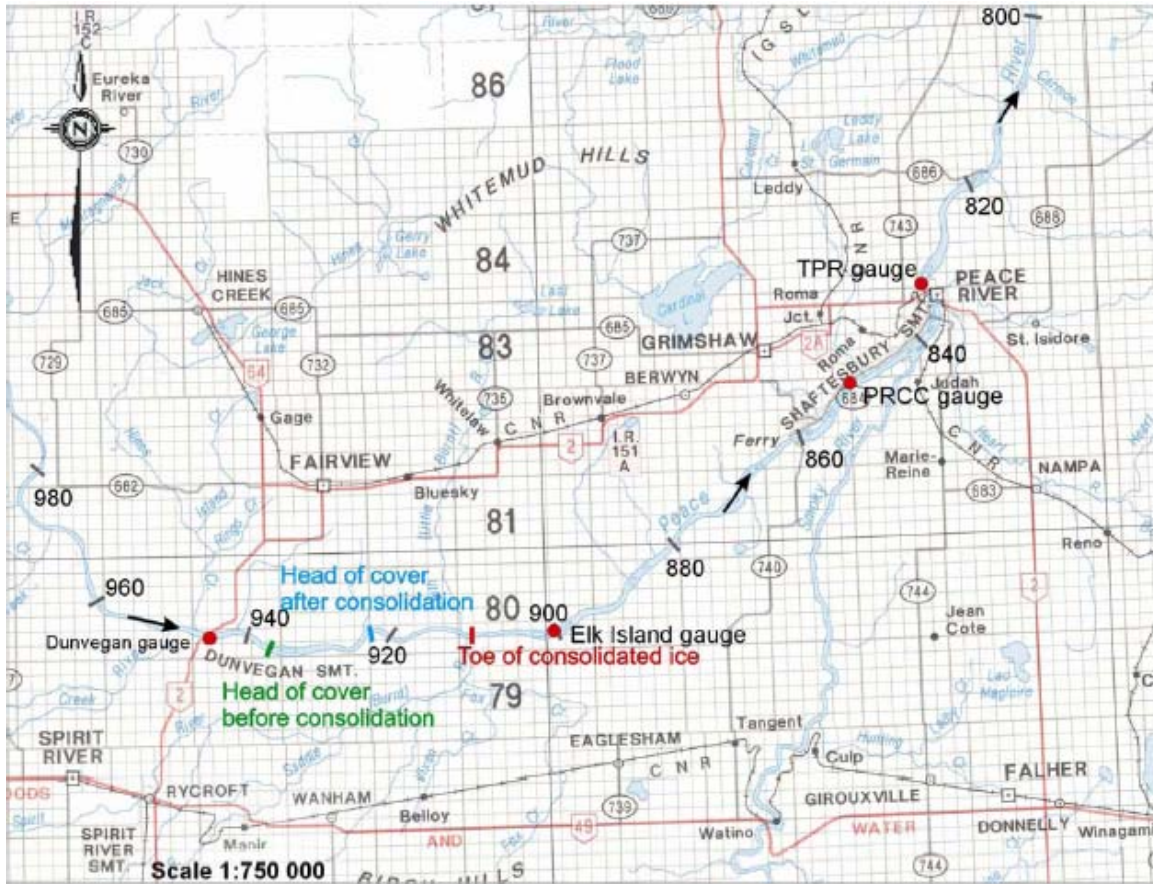


Figure 1. Study area showing gauge locations and ice front locations (TPR = Town of Peace River; PRCC = Peace River Correctional Centre). From Andres et al. (2003).

2. Background Information

As described by Andres et al. (2003), the collapse began at ~ 1930 h on Feb 27, 2001, after the newly-formed ice cover had advanced upstream to within a few kilometres of Dunvegan, and lasted for ~ 6 hours. The resulting consolidation compressed 27 km of the original ice cover into 13 km of a thickened ice accumulation (Fig. 1). The pre-collapse discharge is estimated as $1600 \text{ m}^3/\text{s}$, based on known releases at the Bennett Dam located some 300 km above Dunvegan, and approximate inflows in the intervening reach of the river.

Andres et al. (2003) used the unsteady flow model CDG1D (Hicks, 1996) to simulate the water levels measured at the three gauges shown in Fig. 1, all located downstream of the collapse and consolidation reach. Although this model was not developed to be used for situations with an ice cover, a pseudo ice-covered condition was simulated by adjusting the open-water roughness to represent the composite roughness of both the bed and the ice cover. Given a dearth of cross

section data, the river was assumed to be a rectangular prismatic channel, having a width of 410 m, and a slope of 0.00028. The upstream boundary condition for the model was specified as an inflow hydrograph at the arbitrarily selected site of the new ice front. By trial-and-error, it was found that fair agreement between model predictions and measured waves could be obtained (Fig. 2) when the inflow hydrograph was given a Gaussian shape with a peak flow of $3850 \text{ m}^3/\text{s}$. The duration of the inflow hydrograph was adjusted to match the outflow volume, which was calculated from known backwater levels along the collapse reach. Once the model has been “calibrated” in this fashion, its output can be further examined and processed to determine flow velocities, discharges, friction slopes, and thence shear stresses at any location downstream of the consolidated accumulation. The shear stress is seminal to considerations of ice cover stability because it governs the hydrodynamic forces that are applied on the ice cover during the passage of the wave.

While the model generates comparable waveforms to the measured ones, the “match” is approximate (Fig. 2), and it is difficult to assess the effects of discrepancies in respective water levels on the aforementioned hydraulic characteristics. Ideally, this question would be addressed by reference to actual data obtained by field measurements. However, such data are not available in this case, and are very difficult to obtain when there is ice on the river.

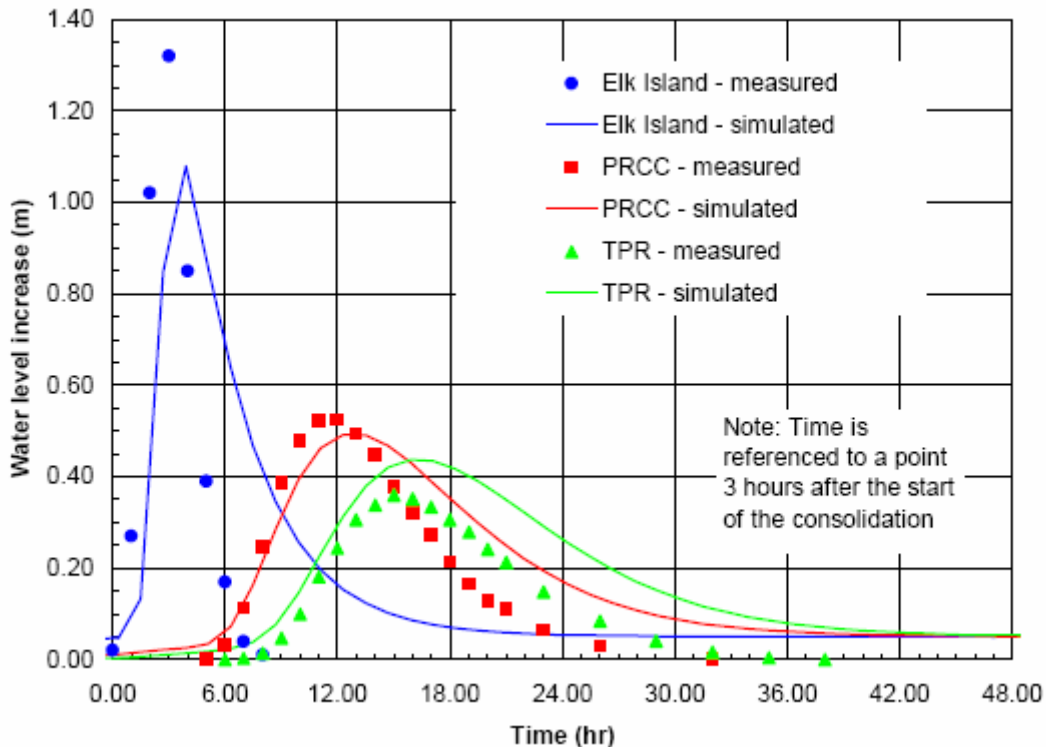


Figure 2. Comparison of measured and simulated stage increases at the three gauge sites downstream of the consolidation area. From Andres et al. (2003).

3. Rising-Limb Analysis

To assess hydrodynamic wave characteristics that are difficult to measure when ice is present, Beltaos and Burrell (2005a), developed an analytical method that utilizes the one-dimensional equations of motion of river flow. By means of partial differentiation and integration, the following equation was obtained for the rising limb of the wave:

$$S_f - S_o \approx \frac{1}{C} \frac{\partial y}{\partial t} \left[1 - a \frac{U^2}{gh} + \frac{C^2}{gh} \left(\frac{(1+a)U}{C} - 1 \right) \right] \quad [1]$$

in which, S_o = unperturbed-flow river slope; S_f = friction slope, defined by the shear stresses that are applied by the flow on the ice cover and channel bed, as well as by the hydraulic radius of the flow; t = time; U = average flow velocity; C = celerity of the waveform; g = gravitational acceleration; y = water depth above the “average” river bed, such that $\partial y/\partial x = -(S_w - S_o)$, with S_w = water surface slope; h = average flow depth, empirically known to vary in proportion to y , such that $h = ay$, with a = site- or reach-specific dimensionless coefficient ($a = 1$ for rectangular channels, and less than 1 for natural bathymetries); and q_o = unperturbed-flow discharge per unit river width.

From the equation of continuity, the average flow velocity U is expressed as (Beltaos and Burrell, 2005a):

$$U = \frac{q_o + \int_{y_o}^y C dy}{h} \quad [2]$$

The integration on the right-hand-side (RHS) of Eq. 2 indicates that C is not a constant, but changes along the waveform, a property that accounts for the looped appearance of the stage-flow variation during the passage of the wave (Beltaos and Burrell, 2005a). The friction slope S_f can be calculated via the Manning resistance relationship:

$$S_f = (nUR^{-2/3})^2 \quad [3]$$

in which n = Manning coefficient of the bed for open-water conditions or of the composite flow for ice-covered conditions; and R = hydraulic radius $\approx h$ or $h/2$, depending on flow condition (open or ice-covered).

In deriving Eq. 1, the frozen-wave approximation was invoked, under which the total derivative Dy/Dt is set equal to zero, so that $\partial y/\partial t + C \partial y/\partial x \approx 0$. This assumption is reasonable along the rising limb of the wave, where the absolute values of the spatial and temporal derivatives are relatively large. It is not reliable in the wave crest region where both derivatives are very small or zero. However, the rising limb is the most dynamic portion of the wave, and it is of most interest because it is here that velocity, flow, and shear stress are highest.

Using Eq. 1, together with Eqs. 2 and 3, the value of $\partial y/\partial t$ can be computed as a function of y , given an assumed variation of C with y . This can be done by specifying the leading-edge celerity (C_L) and the value at the wave peak (C_P), in conjunction with an interpolation function. For the latter, a structure that has been suggested by analysis of the available data is as follows:

$$C = C_P + (C_L - C_P) \exp \left\{ -m \left(\frac{h - h_o}{h_p - h} \right) \right\} \quad [4]$$

in which m = dimensionless interpolation coefficient that may vary from site to site; and h_o , h_p refer to unperturbed- and and peak-stage conditions respectively. The empirical finding that $C_L > C_P$ is reflected in the structure of Eq. 4 (Beltaos and Burrell 2005b).

Consequently, $\partial y/\partial t$ can be determined from Eq. 1 as a function of y for a large number of incremental values of y that represent the range y_o to y_{peak} . For the N^{th} depth (or elevation) interval, Δy , a corresponding time increment is calculated as

$$\Delta t_N = \frac{\Delta y_N}{\frac{1}{2} \left[\left(\frac{\partial y}{\partial t} \right)_{N-1} + \left(\frac{\partial y}{\partial t} \right)_N \right]} \quad [5]$$

By summing the time increments, a set of time values can be applied to any selected set of elevations or depths. The resulting relationship can be compared with the rising limb of the measured wave, and the input parameters (C_L , C_P and m) adjusted until agreement is optimized. There is some ambiguity at the very beginning of the rising limb (or leading edge), where $y \rightarrow y_o$ and $S_f \rightarrow S_o$, resulting in implausibly high values for Δt . This difficulty is circumvented by starting the integration shortly after the arrival of the leading edge, when y is still close to, but perceptibly higher than y_o . Because the frozen-wave approximation is not likely to apply near the peak of the wave, a “match” between measured and calculated y - t variations is considered satisfactory if it applies to the main portion of the rising limb, even if there is no agreement near the wave crest.

The computational procedure can be easily programmed and input parameters (C_L , C_P , and m) can be varied until the calculated flow depths on the rising limb of the wave coincide with the measured ones. Once the optimum values of the input parameters have been selected, it is possible to determine other important hydraulic parameters of the surge, such as instantaneous discharge, average flow velocity, and flow shear stresses. Beltaos and Burrell (2005a) applied the rising-limb analysis method (RLAM) to several measured waveforms that resulted from releases of river ice jams with good results. While it was not possible to fully corroborate the method by measuring directly the velocity and discharge, the leading-edge and peak-stage celerities deduced by RLAM were within the ranges dictated by average values between sites where the waveforms were measured.

4. Application to Measured Waves

Following Andres et al. (2003), the study reach of Peace River is approximated by a rectangular prismatic channel, 410 m wide, with a slope of 0.28 m/km. The composite Manning coefficient is taken as 0.03, a value that has been found to describe the average under-ice flow during the freeze-up period at TPR and applies as well upstream of that location. At the time of the collapse, the aggregate thickness of the ice cover would have been 2 to 2.5 m. Because of the assumed rectangular cross-section of the channel, the presence of the ice cover does not influence the calculated stages, beyond the addition of a constant value. Even this effect disappears, however, when waveforms are expressed in terms of rise above the unperturbed water level.

Application of the analytical method to the measured waves resulted in the comparisons shown in Fig. 3. The agreement between measured and calculated rising limbs is very good, except in the vicinity of the wave crest. The selected RLAM parameters, C_L , C_P , and m , are summarized in Table 1. Though it is not possible to determine corresponding point-values of observed celerities, one can examine average values between gauge sites. The latter are summarized in Table 2 and are seen to be comparable to the values determined via RLAM (Table 1).

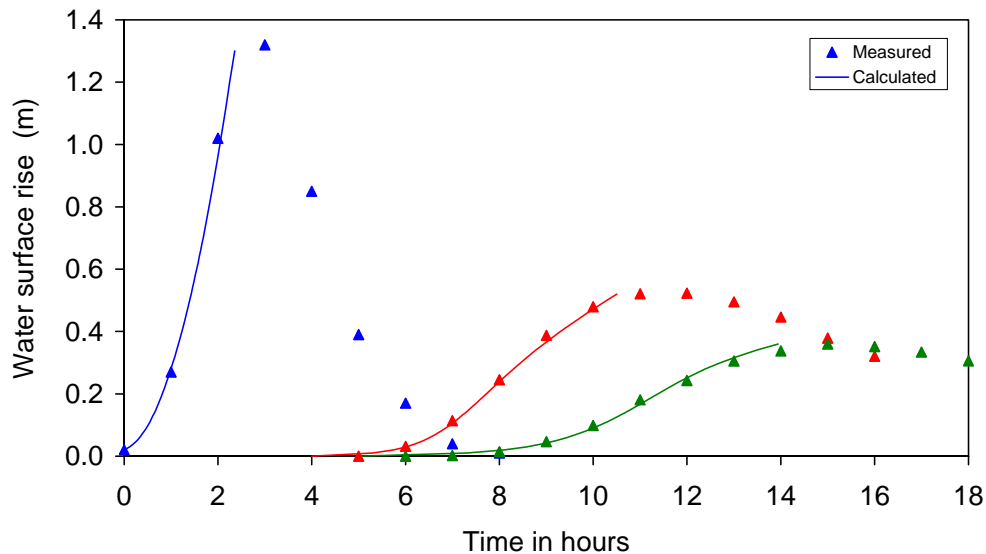


Figure 3. Comparison between measured waves at the three gauging stations and rising-limb portions calculated with the analytical method.

Previous work has shown that celerity decreases with distance traveled (Beltaos and Burrell, 2005b), and this feature is also exhibited by the values in Tables 1 and 2. The trend is further supported by the relationships between respective pairs: for instance, the Elk Island point values (Table 1) are greater than the respective average values between Elk Island and PRCC (Table 2);

the PRCC point values are smaller. At the same time, the PRCC point values are greater than the average values between PRCC and TPR, which in turn are greater than the point values at TPR.

The maximum flows (Q_{max}) determined by the numerical model and by RLAM are very similar at the two downstream gauge sites, but there is significant discrepancy at Elk Island where the numerical model suggests a 20% lower flow. The discrepancy could be related to: (a) analytical over-prediction of stages near the peak (Fig. 3) and (b) model under-prediction within the entire rising limb (Fig. 2). To test this hypothesis, RLAM was applied directly to the model-generated waves, and the respective flow comparisons are illustrated in Fig. 4.

Table 1. Results of application of RLAM to the measured waveforms

Location	m	C_L (m/s)	C_P (m/s)	Q_{max} (m^3/s)	τ_{max} (Pa)	Q_{max} (m^3/s) (from numerical model)
Elk Island	8	3.50	2.50	3080	10.9	2500
PRCC	1.5	2.70	1.53	2110	7.2	1970
TPR	0.5	2.32	1.25	1970	6.8	1930
Downstream Boundary (unperturbed)	NA	NA	NA	1700	6.0	NA

Table 2. Average celerities deduced from measured waves

Reach	C_L (m/s)	C_P (m/s)
Elk Island to PRCC	2.8	1.6
PRCC to TPR	2.5	1.4

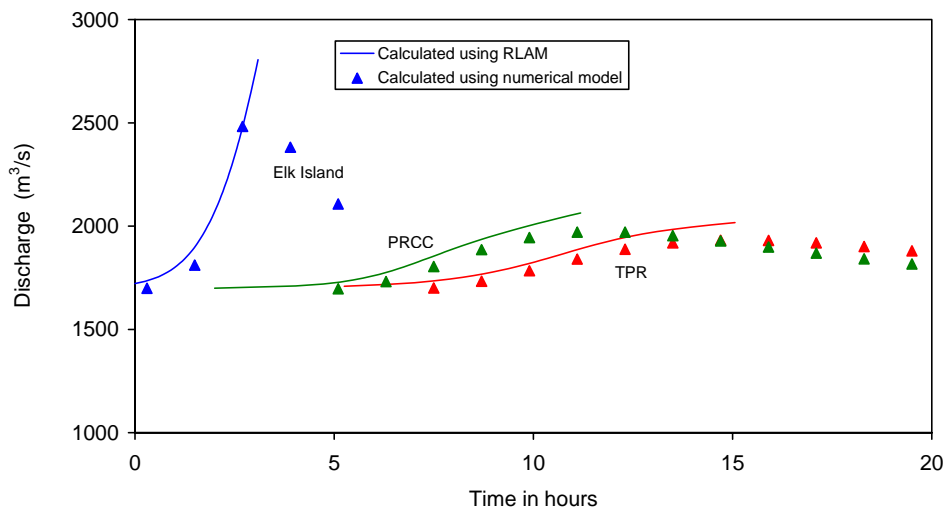


Figure 4. Flow comparisons at the three gauging stations when RLAM is applied to model-generated waves.

Agreement is generally very close. The analytical method still yields a higher peak flow ($\sim 2800 \text{ m}^3/\text{s}$) than the model ($\sim 2500 \text{ m}^3/\text{s}$), but the difference is now halved (from 600 to $300 \text{ m}^3/\text{s}$). Consequently, the best estimate of actual peak flow for Elk Island becomes $\sim 2800 \text{ m}^3/\text{s}$.

5. Ice Cover Stability at Elk Island

The ice cover had advanced past Elk Island sometime between Feb 20 and Feb 23, most likely on Feb 22. During the five day period between then and the consolidation, the mean daily air temperature dropped to as low as $-23.5 \text{ }^\circ\text{C}$ and averaged about $-17 \text{ }^\circ\text{C}$. Environment Canada reported 0.6 cm of snowfall over a two day period between Feb 22 and Feb 23 at the Peace River airport. From considerations of the air temperatures and the snow fall, the thermal (solid) ice thickness at Elk Island was calculated to be between 0.25 and 0.35 m, depending on the adopted porosity of the frazil and the thermal conductivity of the snow cover.

Andres et al. (2003) noted that a stage increase of 1.3 m at Elk Island was insufficient to dislodge the newly formed ice cover. The stage rise represents 3.7 to 5.2 ice thicknesses, which could be sufficient to initiate breakup on certain rivers (Beltaos, 1990). However, this simple criterion that relates the onset of breakup to the ratio of stage rise to ice thickness is empirical, site-specific, and does not take into account local river morphology and forces applied on the ice cover. A more general physically-based criterion that reflects the local channel characteristics has been proposed by Beltaos (1997). Its efficacy has been tested at eight sites on several Canadian rivers (Beltaos, 2004). The criterion is formulated as

$$\Phi_B \equiv \frac{8(W_B - W_i) \varpi_i m^2}{(m - 0.50) h_o} = \beta \sigma_{fo} \left(\frac{\sigma_f h}{\sigma_{fo} h_o} \right) = \beta \sigma_{fo} f(S_5) \quad [6]$$

in which Φ_B represents the multi-variable quantity on the LHS of the equation and has units of stress; W_B = water surface width at the stage at which the breakup is initiated; W_i = width of ice cover which is the river width at freeze-up minus the width of the side strips caused by hinge cracking prior to breakup; h , σ_f = ice cover thickness and flexural strength respectively, while the suffix “o” denotes initial values, just before thermal deterioration begins; m = radius of channel curvature divided by ice cover width; ϖ_i = downslope force per unit area applied on the ice cover by its own weight and by flow shear; and β = dimensionless coefficient, expected to be between 0.3 and 1.5 – measurable quantities only permit assessment of the product $\beta \sigma_{fo}$.

The ratio $\sigma_f h / \sigma_{fo} h_o$ quantifies the reduction in ice “competence” due to thermal deterioration during the pre-breakup period. This process involves reductions in both ice thickness via top and bottom melt, and in strength, due to penetrating solar radiation and preferential melting at crystal boundaries. It is difficult to predict such effects, however, owing to complexities introduced by the snow cover and its changing reflective/absorptive properties as melt progresses (Prowse and Marsh, 1989). Consequently, the “competence” ratio has been expressed as an empirical function of S_5 , the

accumulated degree-days above a base temperature of -5°C (Bilello, 1980). By definition, $f(S_5) = 1$ when $S_5 = 0$. Eq. 6 does not apply to thermal breakup events, but this is not a concern in this case study, as the ice cover was dislodged with minimal, if any, thermal deterioration. An average value for $\beta\sigma_{fo}$ in Eq. [6] would be ~ 90 kPa (Beltaos, 2004). In the present case, a likely value for ice thickness is 0.3 m (the average of the calculated range of thickness). Moreover, $h = h_o$ and $\sigma_f = \sigma_{fo}$ since the consolidation occurred in mid-winter without thermal deterioration of the ice cover (equivalent to setting $S_5 = 0$ and $f(S_5) = 1$).

For an ice cover that comprises a solid ice layer underlain by a porous deposit of ice floes and slush, the driving stress, ϖ_i , can be expressed as:

$$\varpi_i = \gamma R_i S_f + \gamma_i h_i S_w + \gamma p h_p S_w + \gamma_i (1 - p) h_p S_w \quad [7]$$

in which γ and γ_i are the unit weights of water and ice, respectively; h_i and h_p are the thicknesses of the thermal and porous ice layers, respectively; and R_i is the hydraulic radius associated with the ice cover, herein estimated as one-half of the flow depth. The first term on the RHS of Eq. [7] represents the flow shear stress, while the sum of the remaining terms expresses the downslope component of the cover's weight per unit area. In the present case, the friction slope S_f and water-surface slope S_w are very nearly equal and can be used interchangeably, though this may not be the case for highly dynamic waves that can result from releases of major ice jams during breakup. For the Elk Island wave, the maximum shear stress is estimated as 10.9 Pa. With a total ice cover thickness of 2 m, and an assumed porosity of 0.5, the value of ϖ_i would be 18.0 Pa.

Channel curvature varies along the river. The greater the curvature, the smaller is the value of m , and the larger the value of $(W_B - W_i) \varpi_i$ would have to be to produce breakup. This is consistent with the known tendency of sharp bends to instigate ice jams. In the vicinity of Elk Island there are three bends having a radius of about 7 river widths, thus a value of $m = 7.0$ was adopted.

The concept of the breakup initiation process embodied in Eq. [6] presupposes the formation of transverse cracks in the ice and the ability for the resulting ice sheets to be dislocated and move downstream as the water surface width increases with rising stage. The quantity $W_B - W_i$ reflects the space that is available on the water surface for lateral movement of the ice sheets so that they can clear planform-imposed constraints and be set in motion. Substituting $\beta\sigma_{fo} = 90$ kPa, $m = 7$, $f(S_5) = 1$, and $\varpi_i = 18.0$ Pa in Eq. 6, the least value of $W_B - W_i$ that could have initiated breakup at Elk Island is calculated to be about 25 m.

For typical breakup conditions, any unconsolidated ice deposits that would have formed at freezeup have largely melted, and the ice cover essentially consists of sheet ice. In that case, $W_B - W_i$ comprises two quantities: (a) the increase in water surface width due to the rising water level and the sloping river banks; and (b) the width of the side strips of ice created when hinge cracks form. Being attached to the banks, the side strips of ice are initially submerged and weakened before they detach and float. By then, they offer no constraint to the movement of the main ice sheet.

If this approach is applied to the present situation, the total width of the side strips can be calculated to be about 9.5 m (Beltaos, 1997), using a solid-ice thickness of 0.3 m, which is the midpoint of

the estimated range of h . The stage-rise effect requires knowledge of local bathymetry. The closest available river cross-section is located some 7 km downstream of Elk Island and is used as a surrogate. For a rise of 1.3 m, the change in width is estimated as 7.4 m, and the quantity $W_B - W_i$ works out to be ~ 17 m. This is less than the required 25 m, and would explain why the Elk Island ice cover remained intact.

However, the situation analyzed herein is not as straightforward. The solid-ice cover was newly formed and underlain by a much thicker unconsolidated accumulation. Local observations and experience indicate that the grounded, shore-fast portions are about 20 m wide on either side of the river. The edge of the shore-fast accumulation becomes a “shear line”, at which the main (middle) portion of the ice cover separates from the shore-fast ice. It is not immediately evident what the value of $W_B - W_i$ should be in this case, but a number of scenarios can be envisioned. In one scenario the shore-fast ice remains attached to the bank and is completely submerged as the water level rises by 1.3 m. The main portion of the ice cover rises by the same amount and moves laterally and downstream against one bank. In this situation $W_B - W_i$ would comprise the width of the shore-fast ice and the stage-related width change – say a total of 20 to 30 m. In another scenario the shore-fast ice is completely detached from the bank and floats up with the ice cover. In this case the change in width would reflect the formation of hinge cracks and the change in stage would be between 15 and 20 m. In a third scenario, the shore-fast ice remains attached to the bank, but rotates upward with the passage of the wave. The rotation angle is very small (3° to 4° at the most) and the net result would be minimal effective increase in width, making ice cover dislodgement unlikely. In fact, in this situation, the ultimate stability of the ice cover may be related to the ability of the shore ice to accommodate a given stage increase without detaching from the bank or breaking apart.

In all but the last scenario, the width difference is close to the limiting value of 25 m, suggesting that the ice cover at Elk Island was on the verge of being dislodged, and likely would have been, if even a moderately higher (increased $W_B - W_i$) and/or steeper (increased ϖ_i) wave had developed at that location. Taking into account wave attenuation with travelled distance, it can be deduced that the downstream limit of the consolidated cover should have been located not far above Elk Island. This was indeed the case, as illustrated in Fig. 1.

Alternatively, one may work with a range of $W_B - W_i$ to determine a corresponding range for the parameter $\beta\sigma_{fo}$, assuming that the Elk Island ice cover was at the limit of its stability. Setting $W_B - W_i = 20$ to 30 m, $h_{io} = 0.25$ to 0.35 m, and $\varpi_i = 18.0$ Pa, Eq. 6 results in $\beta\sigma_{fo} = 62$ to 130 kPa, which is consistent with the range defined by data on other rivers for conventional breakup conditions (Beltaos 2004).

The above findings suggest that Eq. 6, which has been developed for conventional breakup conditions, may be also relevant in the case of winter consolidation of an ice cover. As the writing of this article was about to be completed, the authors came across data from a more extensive consolidation event on the Peace River, which occurred near Dunvegan on January 30, 2004 (Jasek et al. 2005 - on this CD). The toe of the resulting jam was located in a relatively straight reach between two bends of well-defined curvature, while the wave passage was recorded at nearby gauge. The present method of analysis was applied to the two bends and indicated ice cover dislodgment at the upstream bend ($W_B - W_i = 17$ m) and stability at the

downstream one ($W_B - W_i = 37$ m). The final position of the toe was most likely determined by the formation and eventual grounding of a rubble front.

6. Summary and Conclusions

The recently developed rising-limb analysis method has been applied to three waveforms that were recorded at respective gauging stations on the Peace River, Alberta, following the collapse and consolidation of 27 km of newly-formed ice cover. The deduced leading-edge and peak-stage celerities decrease with distance traveled by the wave, in accordance with previous findings on other rivers. The analysis furnishes point values of celerity which themselves cannot be directly compared with observation, because only the average celerity between gauging stations can be deduced from the recorded waveforms. However, the decreasing trend in celerity suggests that a point value at a given station should exceed the average value to the downstream station and be less than the average value to the upstream one. The analytically deduced celerities conform to these inequalities for all three measured waves and gauging stations.

In general, analytical estimates of peak wave discharge are very close to those obtained earlier by application of a one-dimensional hydrodynamic numerical model. There is a 20% discrepancy with respect to the Elk Island wave, which was shown to have been caused by both analytical over-prediction near the crest and model under-prediction of the entire rising limb.

The analytical method also furnishes peak shear stresses, which can be used to quantify the stability of the ice cover. At Elk Island, the peak shear stress was almost double the unperturbed-flow value. Taking into account the downslope component of the ice cover, a physically-based breakup-initiation criterion was applied to the Elk Island site. It was calculated that the wave-generated forces at Elk Island were insufficient to dislodge the ice cover, which is consistent with the observed ice cover stability at that site and downstream. At the same time, it was noted that a moderately steeper and higher wave might have been able to dislodge the ice cover, which is also consistent with the observed proximity of the upstream end of the intact ice cover.

References

- Andres, D., Van Der Vinne, G., Johnson, B., and Fonstad, G. 2003. Ice consolidation on the Peace River: release patterns and downstream surge characteristics. Proceedings (CD format), 12th Workshop on the Hydraulics of Ice Covered Rivers, CGU HS Committee on River Ice Processes and the Environment, Edmonton, AB, June 19-20, pp. 319-330.
- Beltaos, S. 1990. Fracture and breakup of river ice cover. *Canadian Journal of Civil Engineering*, 17(2): 173-183.
- Beltaos, S. 1997. Onset of river ice breakup, *Cold Regions Science and Technology*, Vol. 25 (3), pp. 183-196.
- Beltaos, S. 2004. Climate impacts on the ice regime of an Atlantic river. *Nordic Hydrology*, Vol 35, No. 2, April 2004, 81-99.
- Beltaos, S. and Burrell, B.C. 2005a. Determining ice-jam surge characteristics from measured wave forms. *Canadian Journal of Civil Engineering*, in press.

- Beltaos, S. and Burrell, B.C. 2005b. Field measurements of ice-jam-release surges. *Canadian Journal of Civil Engineering*, in press.
- Bilello, M.A. (1980). Maximum thickness and subsequent decay of lake, river and fast sea ice in Canada and Alaska, U.S. Army, Cold Regions Research and Engineering Laboratory, Report 80-6, Hanover, New Hampshire, USA, 160 pp.
- Hicks, F.E. 1996. Hydraulic flood routing with minimal channel data: Peace River, Canada. *Canadian Journal of Civil Engineering*. Vol. 23, No. 2 pp. 524-535.
- Jasek, M., Andres, D. and Fonstad, G. 2005. Field and Theoretical Study of the Toe Region of a Dynamic Freeze-up Ice Jam. Proceedings (CD format), 13th Workshop on the Hydraulics of Ice Covered Rivers, CGU HS Committee on River Ice Processes and the Environment, Hanover, NH, USA, September 15-16.
- Neill, C.R. and D. Andres. 1984. Freeze-up flood stages associated with fluctuating reservoir releases. Third International Specialty Conference on Cold Regions Engineering, CSCE/ASCE, Edmonton, Canada.
- Prowse, T.D. and Marsh, P. 1989. Thermal Budget of River Ice Covers During Breakup, *Canadian Journal of Civil Engineering*, Vol. 16, No. 1, pp. 62-71.
- Wigle, T., Doyle, P., Fonseca, F., Mark, H., Parmley, L., Raban, R., and Robert, S. 1990. Optimum Operation of Hydroelectric plants during the ice regime of rivers - A Canadian experience. Prepared by a Task Force of the Subcommittee on Hydraulics of Ice-Covered Rivers, National Research Council of Canada, NRCC 31107, Ottawa, Canada.